



## Kinetics of permeate flux decline and fouling mechanism characterization of colloidal system ultrafiltration: experimental and modeling study

Seyed M.A. Razavi\*, Ali Alghooneh, Fataneh Behrouzian

*Division of Food Engineering, Department of Food Science and Technology, Ferdowsi University of Mashhad (FUM), P.O. Box 91775-1163, Mashhad, Iran, Tel. +98 51 38805763; Fax: +98 51 38763842; emails: s.razavi@um.ac.ir (S.M.A. Razavi), ali.alghooneh@gmail.com (A. Alghooneh), fbehrouzian@yahoo.com (F. Behrouzian)*

Received 5 October 2017; Accepted 29 December 2017

---

### ABSTRACT

Herein, three kinetic models were employed to describe the flux dynamics in terms of the initial flux, flux decline extent, flux decline rate and steady-state flux during crossflow ultrafiltration of skim milk. Homographic kinetic model as the best approach was employed for dynamic modeling of permeate flux of skim milk ultrafiltration at different feed flow rates (FRs), transmembrane pressures (TMPs), temperatures, pH and NaCl levels. All fouling mechanisms presented during the ultrafiltration but dominated by complete blocking. Also, fouling mechanisms were analyzed using Hermia's models. Cake layer showed the highest percentage increase per 1 bar increase in TMP (in the range of 0.3–1 bar), 0.01% increase in NaCl concentration (0–0.12% w/w), 0.1 unit decrease in pH (5.60–6.00), and 1 L/min decrease in FR (30–46 L/min) among other fouling mechanisms.

*Keywords:* Colloid; Dynamic modeling; Flux; Fouling; Kinetics; Semi-empirical; Ultrafiltration

---

### 1. Introduction

Crossflow ultrafiltration (UF) is a well-established procedure with a wide range of industrial applications in the food industry, biotechnology, pharmaceutical industry, water and waste-water treatment, especially for processing of colloidal suspensions, for example, milk system. Milk is a complex system and also highly polydisperse with particles having different charges and a wide range of sizes, which makes the membrane separation practicable. Milk UF depends on hydrodynamic and physicochemical operating conditions, such as TMP, crossflow velocity, temperature, ionic strength and pH [1,2]. Evaluation of the range and significance of the process factors during UF of skim milk is beneficial to test the possibility of controlling UF processes by means of operating conditions and to select engineering means to solve the problem of flux decline.

Experimental crossflow filtration studies involving colloidal suspensions clearly show a relatively rapid flux

decline rate at the start of the filtration, followed by a more gradual decline, until a steady-state flux is approached [3]. The calculation of the initial flux ( $J_0$ ) of any membrane separation systems is an important task in characterizing its transport performance [4]. In the case of milk UF researches, it has become clear that the methods for determining the  $J_0$  may lack in reliability. In addition, the origin of steady-state flux ( $J_\infty$ ) (i.e., the flux in stationary condition after long enough time) is not well conceived.  $J_\infty$  was originally assigned to factors such as cake erosion, deposit removal or back flux. Depending on system conditions and physicochemical properties of fluent, the gradual decline stage can last from minutes to several hours. So it is important to make it clear, how the system variables influence the transient behavior of permeate flux such as rate and extent of flux reduction [5]. Modelling is essential for designing of a new process and developing a better insight of the present process [6]. There are many studies focused on theoretical models, however, they have failed to accurately predict permeate flux decline with time without using experimental data to estimate at least one of their model parameters. Therefore, many design

---

\* Corresponding author.

procedures become empirical and system specific. Although empirical models are very precise, they cannot adequately explain the flux decline/fouling mechanisms involved in membrane processes. Because of the unsatisfactory prediction of the conventional models, there is always a need for alternative methods. Semi-empirical models whose parameters have physical meaning are an appropriate solution [7]. In this research, three semi-empirical models were employed which could help us to understand the mechanisms of permeate flux decline in UF of colloidal systems such as skimmilk.

The main barriers to implementing UF process would be fouling and concentration polarization [8]. It is important to study fouling mechanisms as it is necessary to establish the most appropriate technique for membrane restoration and the operational strategies for lessening the membrane fouling. The deposition process followed several mechanisms. All of these patterns were described by blocking filtration law which consisted of complete pore blocking, standard pore blocking, intermediate pore blocking and cake filtration. Hermia's model offered an analytical description of all four blocking mechanisms. There have been numerous studies in the literature that analyzed fouling using Hermia's model in crossflow filtration [8]. The literature has demonstrated that Hermia's models can accurately predict permeate flux decline in colloidal suspensions filtration at different experimental conditions [9].

Determining the optimum operating conditions to minimize fouling and obtaining a model to predict permeate flux decline with time are key steps with immense importance in UF processes of colloidal systems. In view of the importance of UF in the dairy industry, the authors investigated the dynamics of crossflow UF of skimmilk as a case study to describe the flux decline kinetics in terms of the initial flux ( $J_0$ ), flux decline extent ( $a$ ), flux decline rate ( $b$ ) and steady-state flux ( $J_\infty$ ) as a function of pH, NaCl concentration, TMP, temperature and feed flow rate (FR) during milk UF. Also, the fouling mechanisms were analyzed using Hermia's model and the effect of changes in processing conditions on membrane-fouling intensity was also studied.

## 2. Modeling

In this study, three kinetic models were employed to analyze the flux dynamics of colloidal system crossflow UF as follows:

### 2.1. Exponential kinetic model

The exponential kinetic model (EKM) applies the mass balance equation during membrane filtration in which the decrease of permeate flux expressed with a differential equation is as follows:

$$\frac{d(J_t - J_\infty)}{dt} + \frac{(J_t - J_\infty)}{t_0} = 0 \quad (1)$$

where  $J_t$  is the permeate flux after time equal  $t$ ,  $J_\infty$  is the equilibrium flux and  $t_0$  is the time constant. The equation can be solved using boundary conditions at  $t = 0$ ,  $J = J_0$  and at  $t \rightarrow \infty$ ,  $J_t = J_\infty$  as follows:

$$J_t = (J_0 - J_\infty)\exp(-kt) + J_\infty \quad (2)$$

where  $k$  (1/s) is the decline rate constant and  $J_0$  is the initial flux of the permeate flux.

### 2.2. N-order kinetic model

It is assumed that the change of flux with time is associated with membrane permeability vanishing. Using the analogy with chemical reactions, we may express the flux decline as:

Unsteady state flux  $\rightarrow$  steady-state flux

In the  $n$ -order kinetic model, the evolution of membrane permeability ( $\delta$ ) with time can be represented by a differential equation as follows:

$$\frac{d\delta}{dt} = -\alpha(\delta - \delta_\infty)^n \quad (3)$$

where  $\alpha$  (1/s) is the decline rate constant,  $n$  is the order of permeability decline and  $\delta_\infty$  is the membrane permeability at the steady-state condition. Eq. (3) can be solved using the boundary conditions at  $t = 0$ ,  $\delta = \delta_0$  and at  $t \rightarrow \infty$ ,  $\delta = \delta_\infty$  as follows:

$$(\delta - \delta_\infty)^n = (n-1)\alpha t + (\delta_0 - \delta_\infty)^{1-n} \quad (4)$$

where  $\delta_0$  is the initial permeability. In order to apply Eq. (4) to permeate flux data, we need to specify a relationship between membrane permeability and permeate flux, so we introduced a dimensionless parameter of  $\delta(t)$  as follows:

$$\delta(t) = \frac{(J - J_\infty)}{(J_0 - J_\infty)} \quad (5)$$

Substituting Eq. (5) from Eq. (4) yields:

$$\left(\frac{J_t - J_\infty}{J_0 - J_\infty}\right)^{1-n} = (n-1)\alpha t + 1 \quad (6)$$

### 2.3. Homographic kinetic model

In this study, a homographic kinetic model (HKM) was developed to simulate the permeate flux, as follows:

$$J_t = J_0 - J_0 \left( \frac{ab \times t}{1 + b \times t} \right) \quad (7)$$

where the constant  $a$  (dimensionless) means to what extent the flux declines during UF process and the constant  $b$  (1/s) is the decline rate of the permeate flux during UF. If  $a = 0$ , the flux does not decline at all ( $J_t = J_0$ ) and if  $a = 1$ , the permeate

flux finally reaches zero. For  $0 < a < 1$ ,  $a$  represents asymptotic value namely steady-state flux (or infinite permeate flux), which can be calculated by Eq. (8):

$$J_{\infty} = J_0(1-a) \quad (8)$$

Same as  $a$  constant, if  $b = 0$  the flux does not decline at all ( $J_t = J_0$ ). Lower value of  $b$  means the slower flux declines but higher  $b$  value expresses a steep descent in permeate flux during UF. It is worth mentioning that with reversing  $b$  constant, a new parameter with an important physical concept is obtained ( $1/b$ ). The flux decline time constant ( $1/b$ ) represents the time necessary to reach 50% of total flux decline.

#### 2.4. Hermia's models adapted to crossflow filtration

In this work, adapted Hermia's models for crossflow UF were used to investigate the fouling mechanisms involved in the UF of milk. Eq. (9) is the general differential equation for Hermia's models [8]:

$$-\frac{dJ_t}{dt} = K(J_t - J_{\infty})J_t^{2-n} \quad (9)$$

where  $n$  is the blocking index. Typical values for the parameter  $n$  are the following:  $n = 2$  for complete blocking,  $n = 3/2$  for standard blocking,  $n = 1$  for intermediate blocking and  $n = 0$  for gel layer formation. The constant  $K$  is a phenomenological coefficient constant that depends on the fouling mechanism. According to the complete blocking model, a solute molecule that settles on the membrane surface blocks a pore entrance completely. This model assumes that the particles do not overlap to others that have previously deposited on the membrane. The intermediate blocking model assumes that each solute is settled on previously deposited solute on the membrane surface and not inside the pores. The standard blocking model considers that solute molecules are smaller than the membrane pore size. So, these molecules can penetrate inside the pores. Cake layer formation model is based on the accumulation of the solutes on the membrane surface in a cake form when the solute molecules are larger than the membrane pores. The integrated forms of Hermia's fouling models are given by Eqs. (10)–(13):

$$J_t = J_{\infty} + (J_0 - J_{\infty}) \exp(-K_c J_0 t) \quad (\text{Complete blocking}) \quad (10)$$

$$J_t = \frac{J_0}{(J_0 + J_0^{0.5} K_s t)^2} \quad (\text{Standard blocking}) \quad (11)$$

$$J_t = \frac{(J_0 J_{\infty} \exp(K_i J_{\infty} t))}{(J_{\infty} + J_0 (\exp(K_i J_{\infty} t) - 1))} \quad (\text{Intermediate blocking}) \quad (12)$$

$$t = \frac{1}{(K_g J_{\infty}^2)} \ln \left( \frac{J_t}{J_0} + \left( \frac{J_0 - J_{\infty}}{J_t - J_{\infty}} \right) - J_{\infty} \left( \frac{1}{J_t} - \frac{1}{J_0} \right) \right) \quad (\text{Gel layer formation}) \quad (13)$$

In the above equations, the subscripts in the constant  $K$  refer to the blocking mechanisms (i.e.,  $c$  for complete blocking,  $s$  for standard blocking,  $i$  for intermediate blocking and  $g$  for gel layer formation).

### 3. Experimental setup

#### 3.1. Material and membrane

Reconstituted skim milk was prepared by addition of medium heat skim milk powder to warm water under the fast stirring condition and employed as the feed. The composition of skim milk powder is presented in Table 1. The polymeric hollow fiber membrane was supplied by Koch Membrane Systems, USA, composed of polyethersulfone, MWCO 10 kDa, providing an effective area of 2.42 m<sup>2</sup> with the capability of operating up to 1.2 bar pressure.

#### 3.2. Filtration setup

A schematic diagram of the pilot-scale UF unit operated in this study is illustrated in Fig. 1. The inlet and the outlet feed pressures were monitored by two pressure gauges which positioned as close to the inlet and the outlet of the membrane as physically possible. The crossflow velocity was controlled by changing the rotation speed of the pump 2. The temperature of feed was continuously controlled by the tubular heat exchanger and monitored by a temperature probe attached to the feed tank during each run. The permeate flux was measured and recorded every 60 s.

#### 3.3. Filtration experiment

The dynamics of the permeate flux was investigated over a period of 130 min. For each run, the feed tank was first recycled with pure water at the specified operating condition to evaluate the pure water flux, and then it was recycled with reconstituted skim milk at the same operating conditions. It is worth mentioning that the cleaning procedure was controlled by water flux measurement at the start and end of each run, the difference between the two measured data checked to be less than 3%–5%, if not fouling was not removed and the cleaning procedure was repeated until the flux returned or the membrane was replaced with a new one. Also, in order to determine the concentration of sodium chloride, the

Table 1  
Average chemical composition of skim milk samples<sup>a</sup>

Component	Average (%)	Range <sup>b</sup>
Protein	2.86	0.14
Fat	0.09	0.01
Lactose	4.73	0.28
Ash	0.77	0.05
Total solids	8.44	0.52
pH	6.54	0.01

<sup>a</sup>Each point is the mean of at least two replicates.

<sup>b</sup>Range indicates the difference between the maximum and minimum values of each component.

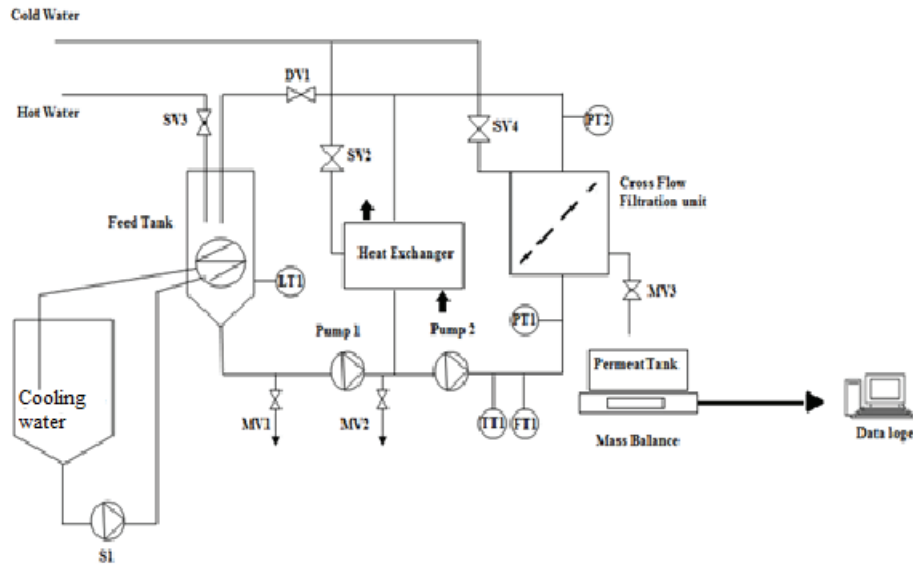


Fig. 1. Schematic diagram of ultrafiltration pilot plant system used in this study.

conductivity of feed was measured by a conductivity meter (Jenway 4010, Bibby Scientific Limited, UK). The kinematic viscosity and density of permeate samples were measured using an Ostwald U-tube capillary viscometer and a 25 mL Pycnometer, respectively.

### 3.4. Data analysis

A completely randomized design was used for statistical analysis. The details on the levels of variables in this design are presented in Table 2. All measurements were conducted at least in triplicate and the data were presented as a mean of each experiment. The experimental data were analyzed by one-way analysis of variance (ANOVA) at 95% confidence level and the means were compared using Duncan test using SPSS 17 (SPSS Inc., Chicago, IL). Curves, data fitting and goodness of fit ( $R^2$ , [coefficients of determination] and RMSE [root mean square error]) were obtained by MATLAB 2010 (7.10.0), using the curve fitting toolbox and trust-region algorithm. The choice of the most appropriate model was based on the highest  $R^2$  and the lowest RMSE values, which calculated by Eqs. (14) and (15), respectively:

$$R^2 = 1 - \frac{SS_{\text{residual}}}{SS_{\text{residual}} + SS_{\text{model}}} \quad (14)$$

$$RMSE = \sqrt{\frac{\sum_{i=1}^N (O_i - T_i)^2}{N}} \quad (15)$$

where  $SS$  is the sum of squares,  $O_i$  is the  $i$ th actual value,  $T_i$  is the  $i$ th predicted value and  $N$  is the number of data. Eventually, a sensitivity analysis based on regression analysis method was conducted to measure the weight of input parameters on permeate flux and fouling mechanisms.

Table 2  
Levels of variables in a completely randomized design used for crossflow ultrafiltration of skim milk

Variables	Run	Operating conditions				
		TMP (bar)	$T$ ( $^{\circ}\text{C}$ )	FR (L/min)	pH	NaCl (%)
TMP (bar)	1	0.30	40	30	6.60	0
	2	0.60	40	30	6.60	0
	3	1.00	40	30	6.60	0
$T$ ( $^{\circ}\text{C}$ )	4	1.00	30	12	6.60	0
	5	1.00	40	12	6.60	0
	6	1.00	50	12	6.60	0
FR (L/min)	7	0.30	50	10	6.60	0
	8	0.30	50	30	6.60	0
	9	0.30	50	46	6.60	0
pH	10	0.30	30	15	5.60	0
	11	0.30	30	15	6.00	0
	12	0.30	30	15	6.60	0
	13	0.30	30	15	6.90	0
	14	0.30	30	15	7.60	0
NaCl (%)	15	1.00	50	56	6.60	0
	16	1.00	50	56	6.60	0.03
	17	1.00	50	56	6.60	0.06
	18	1.00	50	56	6.60	0.12

TMP, transmembrane pressure;  $T$ , temperature; FR, feed flow rate.

## 4. Result and discussion

### 4.1. Model selection

In describing the flux pattern, although all used models indicated high  $R^2$  and low value of RMSE, from the point of being in better agreement with the experimental data,

the HKM model ( $R^2 > 0.93$  and  $RMSE < 0.04$ ) did the best (Table 3). Furthermore, the fitness of this model was considerably better than theoretical and some other empirical models [10–12]. The results of fitting the HKM model to the experimental data at different TMPs, temperatures, FRs, pHs and ionic strengths are shown in Figs. 2–6, respectively. HKM model contains only two constants which are directly related to the curve shape features. This enables simple comparison between the shape characteristics of different model curves. Beside excellent ability of the HKM model to describe the experimental flux–time data, the model parameters (flux decline extent [ $a$ ], flux decline rate [ $b$ ], steady-state flux [ $J_{\infty}$ ] and initial flux [ $J_0$ ]) were of immense practical significance in determining the flux behavior kinetic, in all the tested conditions, which would be discussed in the following sections. Results showed that permeate flux dramatically decreased within the first 15 min of UF operations at all tested conditions (Figs. 2–6). It has been proposed that at the beginning of the operation, the flux decline is due to some kind of pore blocking, followed by the slower flux decline at later stages attributed to cake layer formation [7].

For all conditions studied, all fouling models satisfactorily fitted the flux–time data as indicated by high  $R^2$  and low RMSE values (Table 4), which suggested that all the fouling mechanisms occurred during the skimmilk UF process. The values of fitted parameters, as shown in Table 5, supported this statement. These fouling mechanisms are reasonable as skimmilk consists of a broad size distribution of albumin, globulins and other types of protein molecules [13]. In addition, the higher  $R^2$  and the lower RMSE for skimmilk samples at all conditions were observed for all the pore blocking models than cake layer model (Table 4). This result

is in agreement with other research works, which found that pore blocking mechanisms dominated membrane fouling during the filtration of proteinaceous solutions [8,14]. The worst predictions were obtained at high crossflow velocities (46 L/min) (run 9, Table 2) by cake layer model (the lowest  $R^2$  and the highest RMSE) and the best fitting was for the same run with intermediate blocking model ( $R^2 = 0.94$  and the lowest RMSE) (Table 3).

#### 4.2. Effect of transmembrane pressure

The modeling results of dynamic permeate flux at various TMP (temperature 40°C, pH = 6.6, FR 30 L/min and 0% NaCl) are demonstrated in Table 6. The range of TMP in this research was in the pressure-dependent zone. With each 0.1 bar increase in TMP in the range of 0.6 to 1 bar,  $J_0$  and  $J_{\infty}$  increased by 7.69% and 4.88%, respectively, which were more prominent than those in the range of 0.3 to 0.6 bar (Table 7). Greater  $J_0$  and  $J_{\infty}$  at higher TMP is attributed to the fact that the UF is a pressure-driven membrane process and increasing TMP enhances the driving force, which induces higher convective mass of particles toward the membrane surface at higher pressures [15]. Results showed that permeate flux declined more rapidly at higher TMP (Table 6). The effect of each 0.1 bar enhancement in the TMP on the increasing of  $1/b$  was more obvious in the range of 0.6–1 bar (6.74%) than at 0.3–0.6 bar (4.71%) (Table 7). This behavior can be explained by the increase in particle deposition rate at higher TMP and formation of a more densely packed cake layer [16]. Similar behavior was observed by Herrero et al. [17] during BSA (*bovine serum albumin*) solution microfiltration. The analysis of blocking mechanism during UF of skimmilk due to the

Table 3

Values of the goodness of fit ( $R^2$  and RMSE) determined for exponential kinetic (EKM),  $n$ -order kinetic (NKM) and homographic kinetic (HKM) models at different operating conditions of skimmilk ultrafiltration

Treatments					EKM		NKM		HKM	
$T$ (°C)	TMP (bar)	pH	FR (L/min)	NaCl (%)	$R^2$	RMSE	$R^2$	RMSE	$R^2$	RMSE
30	1	6.6	12	0	0.89	0.06	0.85	0.07	0.96	0.01
40	1	6.6	12	0	0.87	0.03	0.86	0.05	0.94	0.02
50	1	6.6	12	0	0.91	0.01	0.92	0.03	0.95	0.02
40	0.3	6.6	30	0	0.91	0.06	0.95	0.01	0.95	0.01
40	0.6	6.6	30	0	0.92	0.03	0.95	0.01	0.94	0.01
40	1	6.6	30	0	0.93	0.06	0.93	0.01	0.92	0.05
30	0.3	5.6	15	0	0.88	0.03	0.87	0.07	0.93	0.04
30	0.3	6	15	0	0.87	0.01	0.85	0.06	0.96	0.01
30	0.3	6.6	15	0	0.87	0.02	0.88	0.05	0.97	0.02
30	0.3	6.9	15	0	0.96	0.02	0.95	0.02	0.96	0.01
30	0.3	7.6	15	0	0.93	0.05	0.95	0.02	0.97	0.01
50	0.3	6.6	10	0	0.91	0.04	0.93	0.02	0.95	0.01
50	0.3	6.6	30	0	0.96	0.02	0.95	0.01	0.97	0.01
50	0.3	6.6	46	0	0.86	0.04	0.88	0.03	0.93	0.01
50	1	6.6	57	0	0.90	0.02	0.89	0.03	0.98	0.02
50	1	6.6	57	0.03	0.85	0.07	0.88	0.04	0.97	0.02
50	1	6.6	57	0.06	0.93	0.02	0.88	0.03	0.96	0.02
50	1	6.6	57	0.12	0.94	0.02	0.93	0.01	0.97	0.02

TMP, transmembrane pressure;  $T$ , temperature; FR, feed flow rate.

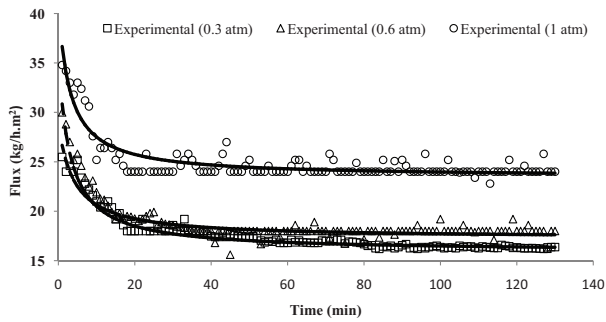


Fig. 2. Dynamic flux curves during skim milk ultrafiltration as a function of transmembrane pressure (temperature 40°C, pH = 6.6, flow rate 30 L/min, 0% NaCl and homographic kinetic model predictions).

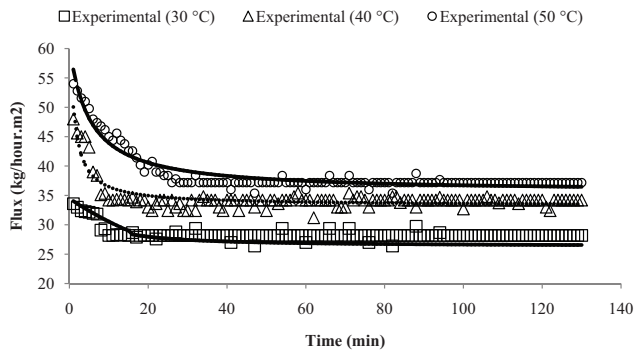


Fig. 3. Dynamic flux curves during skim milk ultrafiltration as a function of temperature (transmembrane pressure 1 bar, pH = 6.6, flow rate 12 L/min, 0% NaCl and homographic kinetic model predictions).

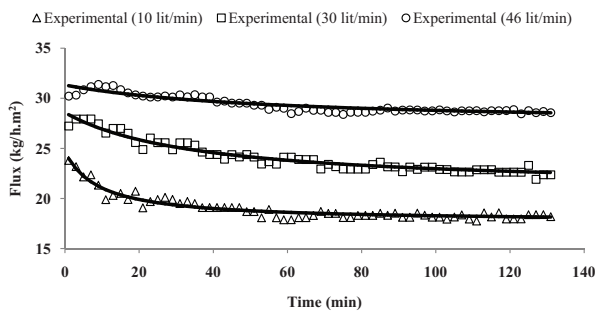


Fig. 4. Dynamic flux curves during skim milk ultrafiltration as a function of crossflow velocity (temperature 30°C, transmembrane pressure 0.3 bar, pH = 6.6, 0% NaCl and homographic kinetic model predictions).

effect of TMP is presented in Tables 4 and 5. The flux decline was more pronounced at higher TMP indicated by higher  $a$  parameter (Table 6), thus the values of Hermia's model parameters at high TMP were higher than those in the low TMP conditions (Table 5). The higher  $K_c$  values than  $K_f$ ,  $K_s$  and  $K_{cf}$  at all TMP levels verified that the complete pore blocking mechanism was the dominant fouling pattern followed by intermediate blocking (Table 5). In intermediate blocking fouling mechanism, the membrane pores are blocked near

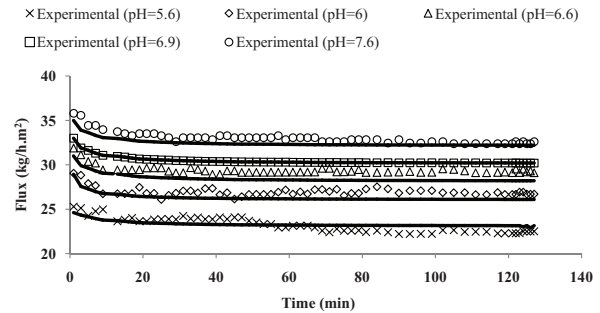


Fig. 5. Dynamic flux curves during skim milk ultrafiltration as a function of pH (temperature 30°C, transmembrane pressure 0.3 bar, flow rate 15 L/min, 0% NaCl and homographic kinetic model predictions).

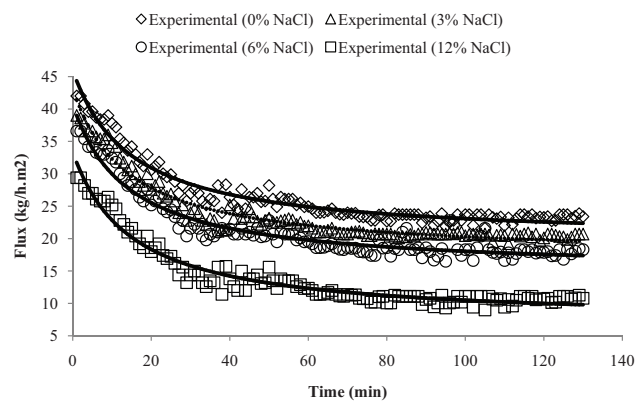


Fig. 6. Dynamic flux curves during skim milk ultrafiltration as a function of NaCl concentrations (temperature 50°C, transmembrane pressure 1.0 bar, pH = 6.6, flow rate 56 L/min and homographic kinetic model predictions).

their entrance to the feed side. However, not all of them are completely blocked. This performance can be expected because the solute molecules were not being completely retained by the membrane, what describes more accurately a real UF process. In addition, with each 0.1 bar increase in TMP in the range of 0.3–0.6 bar and 0.6–1 bar,  $K_{cf}$  increased by 40.67% and 17.03%, respectively, which showed the highest influence of TMP on gel layer formation among other fouling mechanisms (Table 7). The cake layer fouling mechanism occurs when solute molecules are unable to enter the membrane pores due to their greater size. Molecular deformation, cake compression and cake layer thickness are the main factors that have an influence on the cake layer resistance. High TMP may result in a high deformation of the molecules, high cake compression and favors the accumulation of solute molecules on the membrane surface [7].

#### 4.3. Effect of temperature

As seen in Tables 6 and 7, the values of  $J_0$  and  $J_\infty$  increased with temperature which were more obvious from 30°C to 40°C (6.41% for  $J_0$  and 9.52% for  $J_\infty$ ) than those from 40°C to 50°C (0.60% for  $J_0$  and 0.68% for  $J_\infty$ ), indicated the main effect of temperature on these parameters was in the former range.

Table 4

Values of the goodness of fit ( $R^2$  and RMSE) determined for Hermia's models at different operating conditions of skim milk ultrafiltration

Treatments					$n = 2$		$n = 1.5$		$n = 1$		$n = 0$	
$T$ (°C)	TMP (bar)	pH	FR (L/min)	NaCl (%)	$R^2$	RMSE	$R^2$	RMSE	$R^2$	RMSE	$R^2$	RMSE
30	1	6.6	12	0	0.96	0.13	0.95	0.33	0.94	0.11	0.93	1.12
40	1	6.6	12	0	0.92	0.23	0.91	0.35	0.91	0.15	0.91	1.18
50	1	6.6	12	0	0.96	0.37	0.97	0.35	0.98	0.15	0.99	1.20
40	0.3	6.6	30	0	0.89	0.26	0.92	0.37	0.94	0.14	0.89	1.02
40	0.6	6.6	30	0	0.92	0.48	0.94	0.29	0.94	0.22	0.85	2.03
40	1	6.6	30	0	0.90	0.26	0.90	0.16	0.90	0.12	0.91	1.02
30	0.3	5.6	15	0	0.97	0.12	0.97	0.16	0.98	0.26	0.82	1.04
30	0.3	6	15	0	0.88	0.17	0.88	0.15	0.89	0.35	0.88	1.03
30	0.3	6.6	15	0	0.93	0.14	0.93	0.23	0.93	0.44	0.84	1.01
30	0.3	6.9	15	0	0.9	0.12	0.91	0.21	0.91	0.23	0.92	1.01
30	0.3	7.6	15	0	0.88	0.13	0.89	0.12	0.90	0.13	0.90	2.01
50	0.3	6.6	10	0	0.89	0.24	0.93	0.15	0.91	0.21	0.88	2.02
50	0.3	6.6	30	0	0.95	0.33	0.96	0.13	0.97	0.15	0.89	1.01
50	0.3	6.6	46	0	0.94	0.11	0.94	0.11	0.94	0.05	0.75	3.01
50	1	6.6	57	0	0.96	0.55	0.97	0.25	0.98	0.45	0.89	1.02
50	1	6.6	57	0.03	0.93	0.24	0.95	0.19	0.96	0.33	0.90	1.01
50	1	6.6	57	0.06	0.91	0.13	0.94	0.41	0.96	0.28	0.89	2.04
50	1	6.6	57	0.12	0.92	0.12	0.95	0.22	0.97	0.57	0.85	2.01

TMP, transmembrane pressure;  $T$ , temperature; FR, feed flow rate.

The impact of temperature on  $J_{\infty}$  was more obvious than on  $J_0$  indicated the greater effect of temperature on the steady-state flux. The increasing trend of  $J_0$  and  $J_{\infty}$  with temperature may have several reasons. At higher temperature, the viscosity of the bulk fluid decreased and the energy of fluid was higher which caused an increase in the diffusion constants of skim milk components. Furthermore, an increase in temperature may cause an increase in the effective pore radius of the membrane [18]. Razavi et al. [11] observed both  $J_0$  and  $J_{\infty}$  increased with the increase of temperature in the range of 30°C–50°C, although, they stated that increase between 40°C and 50°C was slight. Eckner and Zottola [18] studied the effect of temperature on flux behavior of skim milk and observed a significant increase in flux with an increase in processing temperature. In addition, as temperature increased, the  $1/b$  parameter decreased (Table 6). Heating in the range of 30°C–40°C was the major factor that affected  $1/b$  among other operational and physicochemical properties with an almost 7.76% reduction per 1°C increase in temperature (Table 7).

With the increase in temperature, the diffusion coefficient of some molecules such as proteins increased and the viscosity of the feed solution decreased, so, resulted in higher rate of deposition on the membrane surface and flux reduction. With increasing the temperature from 30°C to 40°C and from 40°C to 50°C, the extent of flux reduction increased by 1.95% and 1.63% per 1°C increase in temperature, respectively (Table 7). This behavior could be due to the low

activation energy of molecules at low temperature, thus, they are adsorbed on the membrane with weak bonding such as hydrogen bonding. However, at high temperature, chemical reactions influence the interaction between solutes and membrane, which resulted in greater flux reduction [6].

The analyses of blocking mechanisms during UF of skim milk due to the effect of temperature showed that at 40°C and 50°C the complete blocking and at 30°C the intermediate blocking dominated throughout the filtration process (Table 5). The increase in the diffusion coefficient of proteins with temperature led to greater penetration into the pores and deposition along the pore walls [19]. On the other hand, due to the solubility reduction of proteins at higher temperature their size increased and the fouling mechanism shifted from intermediate to complete blocking. The standard and complete fouling coefficients increased with temperature, whereas, the intermediate fouling coefficient behaved adversely (Table 5). Razavi et al. [11] found that the amount of total resistance increased with increasing temperature during the skim milk UF.

#### 4.4. Effect of crossflow velocity

According to Table 6, the parameters of  $J_0$  and  $J_{\infty}$  increased with increase in FR, more obvious for  $J_{\infty}$  than  $J_0$ , suggested the greater effect on steady-state fouling reduction. A similar result for the effect of flow rate on the  $J_0$  was observed by

Table 5  
Parameters of fitted Hermia’s model from the study of the effect of physiochemical and operating parameters upon membrane fouling

T (°C)	TMP (bar)	pH	FR (L/min)	NaCl (%)	$K_c$ (s <sup>-1</sup> )	$K_s$ (s <sup>-0.5</sup> m <sup>-0.5</sup> )	$K_i$ (m <sup>-1</sup> )	$K_{cf}$ (s m <sup>-2</sup> )
30	1	6.6	12	0	0.0039	0.0032	0.0051	6.1523 × 10 <sup>-5</sup>
40	1	6.6	12	0	0.0047	0.0041	0.0042	7.7215 × 10 <sup>-5</sup>
50	1	6.6	12	0	0.0123	0.0064	0.0018	0.0002
40	0.3	6.6	30	0	0.0028	0.0012	0.0022	0.3218 × 10 <sup>-5</sup>
40	0.6	6.6	30	0	0.0036	0.0016	0.0028	0.7145 × 10 <sup>-5</sup>
40	1	6.6	30	0	0.0049	0.0021	0.0036	1.2015 × 10 <sup>-5</sup>
30	0.3	5.6	15	0	0.0086	0.0029	0.0077	3.1280 × 10 <sup>-5</sup>
30	0.3	6	15	0	0.0036	0.0021	0.0027	0.8173 × 10 <sup>-5</sup>
30	0.3	6.6	15	0	0.0021	0.0019	0.0017	0.7145 × 10 <sup>-5</sup>
30	0.3	6.9	15	0	0.0018	0.0015	0.0011	0.4231 × 10 <sup>-5</sup>
30	0.3	7.6	15	0	0.0014	0.0012	0.0009	0.3142 × 10 <sup>-5</sup>
50	0.3	6.6	10	0	0.0039	0.0025	0.0019	1.1231 × 10 <sup>-5</sup>
50	0.3	6.6	30	0	0.0021	0.0017	0.0015	0.8231 × 10 <sup>-5</sup>
50	0.3	6.6	46	0	0.0009	0.0013	0.0007	0.2143 × 10 <sup>-5</sup>
50	1	6.6	57	0	0.0034	0.0011	0.0018	0.9124 × 10 <sup>-5</sup>
50	1	6.6	57	0.03	0.0038	0.0012	0.0019	1.2315 × 10 <sup>-5</sup>
50	1	6.6	57	0.06	0.0045	0.0013	0.0022	1.7321 × 10 <sup>-5</sup>
50	1	6.6	57	0.12	0.0086	0.0016	0.0027	6.2142 × 10 <sup>-5</sup>

$K_c$ ,  $K_s$ ,  $K_i$  and  $K_{cf}$  are Hermia’s model constants for complete blocking, standard blocking, intermediate blocking and gel layer formation, respectively.

Table 6  
Parameters of the homographic kinetic model (HKM) determined for different operating conditions of skim milk ultrafiltration\*

Variable	Operating conditions					HKM parameters			
	TMP (bar)	T (°C)	FR (L/min)	pH	NaCl (%)	$a$	1/b (min)	$J_0$ (kg/h × m <sup>2</sup> )	$J_\infty$ (kg/h × m <sup>2</sup> )
TMP (bar)	0.30	40	30	0	6.60	0.40 <sup>a</sup> ± (0.01)	42.88 <sup>c</sup> ± (1.32)	26.98 <sup>a</sup> ± (2.04)	17.22 <sup>a</sup> ± (0.22)
	0.60	40	30	0	6.60	0.45 <sup>b</sup> ± (0.02)	35.67 <sup>b</sup> ± (1.19)	31.67 <sup>b</sup> ± (2.56)	19.74 <sup>b</sup> ± (1.29)
	1.00	40	30	0	6.60	0.55 <sup>c</sup> ± (0.01)	29.98 <sup>a</sup> ± (1.36)	38.89 <sup>c</sup> ± (2.23)	25.08 <sup>c</sup> ± (0.27)
T (°C)	1.00	30	12	0	6.60	0.41 <sup>a</sup> ± (0.02)	19.77 <sup>c</sup> ± (2.53)	34.81 <sup>a</sup> ± (0.86)	15.07 <sup>a</sup> ± (1.72)
	1.00	40	12	0	6.60	0.49 <sup>b</sup> ± (0.03)	11.13 <sup>b</sup> ± (1.15)	57.13 <sup>b</sup> ± (1.78)	29.41 <sup>b</sup> ± (1.05)
	1.00	50	12	0	6.60	0.57 <sup>c</sup> ± (0.02)	5.04 <sup>a</sup> ± (2.82)	60.60 <sup>c</sup> ± (1.62)	31.41 <sup>c</sup> ± (2.01)
FR (L/min)	0.30	50	10	0	6.60	0.31 <sup>c</sup> ± (0.02)	7.06 <sup>a</sup> ± (1.57)	25.51 <sup>a</sup> ± (1.17)	17.70 <sup>a</sup> ± (1.72)
	0.30	50	30	0	6.60	0.24 <sup>b</sup> ± (0.01)	17.61 <sup>b</sup> ± (2.33)	28.80 <sup>b</sup> ± (0.57)	22.94 <sup>b</sup> ± (1.05)
	0.30	50	46	0	6.60	0.13 <sup>a</sup> ± (0.01)	28.08 <sup>c</sup> ± (3.41)	31.40 <sup>c</sup> ± (0.37)	27.32 <sup>c</sup> ± (2.01)
pH	0.30	30	15	0	5.60	0.17 <sup>c</sup> ± (0.02)	17.76 <sup>abc</sup> ± (1.64)	26.68 <sup>a</sup> ± (1.45)	21.02 <sup>a</sup> ± (1.96)
	0.30	30	15	0	6.00	0.14 <sup>bc</sup> ± (0.02)	19.26 <sup>c</sup> ± (1.57)	30.65 <sup>b</sup> ± (1.52)	25.81 <sup>b</sup> ± (2.12)
	0.30	30	15	0	6.60	0.12 <sup>b</sup> ± (0.02)	15.46 <sup>a</sup> ± (1.98)	31.95 <sup>b</sup> ± (2.33)	27.86 <sup>b</sup> ± (2.74)
	0.30	30	15	0	6.90	0.09 <sup>a</sup> ± (0.01)	18.69 <sup>bc</sup> ± (0.77)	37.23 <sup>c</sup> ± (1.75)	33.42 <sup>c</sup> ± (1.38)
	0.30	30	15	0	7.60	0.07 <sup>a</sup> ± (0.01)	16.29 <sup>ab</sup> ± (0.73)	40.50 <sup>c</sup> ± (1.01)	37.06 <sup>d</sup> ± (1.55)
NaCl (%)	1.00	50	56	0	6.60	0.56 <sup>a</sup> ± (0.03)	14.93 <sup>c</sup> ± (2.65)	46.25 <sup>c</sup> ± (1.51)	23.60 <sup>a</sup> ± (0.93)
	1.00	50	56	0.03	6.60	0.60 <sup>a</sup> ± (0.02)	12.72 <sup>bc</sup> ± (2.32)	43.88 <sup>c</sup> ± (1.58)	20.12 <sup>b</sup> ± (0.33)
	1.00	50	56	0.06	6.60	0.64 <sup>b</sup> ± (0.01)	10.38 <sup>ab</sup> ± (1.37)	40.68 <sup>b</sup> ± (1.82)	14.82 <sup>c</sup> ± (0.93)
	1.00	50	56	0.12	6.60	0.79 <sup>c</sup> ± (0.03)	7.92 <sup>a</sup> ± (1.71)	34.48 <sup>a</sup> ± (1.73)	5.02 <sup>d</sup> ± (2.22)

\* $a$ , Flux decline extent; 1/b, flux decline time constant;  $J_0$ , initial flux,  $J_\infty$ , steady-state flux.

<sup>a-d</sup>Means followed by the same letters in the same column, for each variable, are not significantly different ( $P > 0.05$ ).

Table 7

Effect of various range of temperature, pH, transmembrane pressure, feed flow rate and NaCl concentrations on the parameters of homographic kinetic and Hermia's models in crossflow ultrafiltration of skimmilk

Parameter	Range	$a$	$1/b$ (min)	$J_0$ (kg/h × m <sup>2</sup> )	$J_{\infty}$ (kg/h × m <sup>2</sup> )	$K_c$ (s <sup>-1</sup> )	$K_s$ (m <sup>-0.5</sup> s <sup>-0.5</sup> )	$K_i$ (m <sup>-1</sup> )	$K_{cf}$ (s m <sup>-2</sup> )
TMP (bar)	0.30–0.60	1.89	-4.71	5.06	2.96	9.52	11.11	9.09	40.67
	0.60–1.00	2.17	-6.74	7.69	4.88	9.72	7.81	7.14	17.03
$T$ (°C)	30–40	1.95	-7.76	6.41	9.52	2.05	2.81	-1.76	2.55
	40–50	1.63	-5.41	0.60	0.68	16.17	5.61	-5.71	15.90
FR (L/min)	10–30	-1.13	5.47	0.64	0.92	-2.31	-1.61	-1.05	-1.33
	30–46	-2.86	3.72	0.56	1.3	-3.57	-1.47	-3.33	-4.62
pH	5.60–6.00	-1.47	2.11	4.84	5.43	-14.53	-6.90	-16.23	-18.46
	6.00–6.60	-2.13	-3.29	0.76	1.32	-6.94	-1.59	-6.17	-1.06
	6.60–6.90	-3.13	3.96	5.26	4.65	-4.76	-7.02	-11.76	-14.91
	6.90–7.20	-3.40	-1.83	1.25	1.55	-3.17	-2.86	-2.59	-3.61
NaCl (%)	0.00–0.03	1.75	-4.93	-1.71	-4.91	3.92	3.03	6.28	11.66
	0.03–0.06	2.22	-5.13	-2.43	-8.78	6.14	2.78	5.26	13.55
	0.06–0.12	3.93	-3.95	-2.54	-11.02	13.18	33.85	3.78	43.40

TMP, transmembrane pressure;  $T$ , temperature; FR, feed flow rate.

Grandison et al. [20]. The percentage of these enhancements was almost the same with each 1 L/min increase in FR in the ranges of 10–30 and 30–46 L/min. The effect of FR on the flux decline could be better observed with paying attention to the  $a$  values which decreased by 1.13% and 2.86% with each 1 L/min increase in FR in the range of 10–30 and 30–46 L/min, respectively (Table 7). These phenomena may be due to that the generated flow field increased the wall shear rate in the neighborhood of the membrane, resulting in improved scouring of the membrane surface. By using higher crossflow velocities, the concentration polarization and thickness of a dense micellar layer decreased, as evidenced by lower  $K_{cf}$  at higher FR (Table 5), which could result from an increase in back diffusion and shear enhanced diffusion, thus helped to achieve higher long-term permeation flux [21]. Hong et al. [16] investigated the effect of crossflow velocity on the behavior of permeate flux in a study on colloidal suspensions and stated that at pseudo-steady state, as the cake layer thickness approached a steady state, the permeate flux slightly increased with increase in shear rate.

The value of  $1/b$  parameter increased with FR, especially in the range of 10–30 L/min (5.47% increase per 1 L/min rise in FR) (Table 7). The increase of  $1/b$  with increasing FR may be because the rate of particle removal was higher than particle deposition. At 10 and 30 L/min FR, the complete blocking mechanism was the main blocking mechanism in skimmilk UF followed by standard blocking mechanism, whereas at 46 L/min the standard blocking was the main blocking mechanism (Table 5).  $K_{cf}$  and  $K_c$  showed the highest reduction per 1 L/min rise in FR in the range of 10–30 and 30–46 L/min among others fouling constants of Hermia's model, respectively. The cake layer thickness is mainly controlled by the rate of deposition of molecules over the membrane surface against the back transport of molecules toward the bulk solution. Lower crossflow velocity favors greater cake layer thickness [7].

#### 4.5. Effect of feed pH

Tables 6 and 7 show that the  $J_0$  and  $J_{\infty}$  significantly increased as the pH of skimmilk increased from 5.60 to 7.60, especially in the range of 6.60–6.90, which showed almost 4.84% and 5.43% increase with each 0.1 pH increase, respectively. This is because of approaching the isoelectric point of main milk proteins, which is below pH = 5.6 [22], and in the isoelectric point, the solubility of milk proteins is at the lowest extent. Ramachandra Rao [23] reported that acid whey had a lower initial flux and higher extent of flux decline than sweet whey and attributed those behaviors to the existence of more ionic calcium in the acidic sample. The  $a$  value decreased with the increase of pH and the highest reduction was observed in the range of 6.90–7.20 (3.40% for each 0.1 pH increase) (Table 7). The decrease in pH would increase the concentration of calcium in the ionic form which may bridge negatively charged proteins to negatively charged membranes causing a more severe decrease in flux [24]. Razavi et al. [12] reported decreasing the pH of skimmilk from 6.43 to 5.97 considerably decreased the  $J_0$  and  $J_{\infty}$ . On the other hand, there was trend without significance in  $1/b$  with pH increasing (Table 6). The casein micelles are stabilized from aggregating by steric and electrostatic stabilization due to  $\kappa$ -casein molecules, so contribute largely to the viscosity of skimmilk [25]. Reduction of pH could induce changes in the physicochemical properties of the casein micelles [26] and reduces the viscosity of skimmilk which could explain the absence of significant trend for the  $1/b$  parameter.

As the pH increased, membrane fouling decreased, consequently, the value of the model parameters was smaller, as expected. In addition, complete blocking was the main blocking mechanism for all pH levels (Table 5). On the other hand, the highest percentage of fouling constant reduction with each 0.1 unit increase in pH was that corresponded to gel layer, which decreased 18.46% at the range of 5.60–6.00,

followed by 16.23% reduction in intermediate blocking at the same pH range (Table 7). Toward lower pH, more proteins and amino acids are charged which are more reactive and increase fouling and gel layer formation. Therefore, the bridge of negatively charged proteins to negatively charged membranes may cause the deposition of milk protein on the surface which could prevent the movement to the permeate side.

#### 4.6. Effect of feed ionic strength

The results indicated that significantly lower  $J_0$  and  $J_\infty$  values at higher NaCl concentration (Table 6), especially in the range of 0.06%–0.12% NaCl, showed 2.54% and 11.02%  $J_0$  and  $J_\infty$  reduction with each 0.01% increase in NaCl concentration, respectively (Table 7). More sensitivity of  $J_\infty$  to NaCl concentration than  $J_0$  could be explained by the fact that, at the start of the filtration, particle deposition is negligible and the intrinsic membrane hydraulic permeability is the determinative factor of resistance to flow. Higher ionic strength decreases the range of repulsive forces among milk compounds and between compounds and the membrane surface [27] and also increases the surface tension of the solution [28]. The increase of the attractive interactions between colloids in the system increases the viscosity of feed; as a result,  $J_0$  decreases [26]. The effect of ionic strength on  $J_\infty$  parameter can be rationalized by concerning that the interparticle distance in the cake layer decreases at higher ionic strengths as a result of a decrease in the range of the electrostatic double layer repulsive forces; accordingly, the cake layer is more densely packed and the resistance to permeate flow increases at steady-state stage [3]. In addition, NaCl makes the exchange between the added monovalent cations ( $\text{Na}^+$ ) and divalent cations ( $\text{Ca}^{2+}$ ). As  $\text{Ca}^{2+}$  is a major factor in the structure of calcium phosphate clusters, which contributes to the rigidity of the casein micelles, NaCl addition may increase micelle size and volume fraction.

The flux decline extent ( $a$ ) significantly increased by the increase in NaCl concentration, more obvious in the range of 0.06%–0.12% NaCl, which increased 3.93% with 0.01% increase in the NaCl concentration (Tables 6 and 7). When the ionic strength increased, the permeate flux decline became more rigorous, and faster approached to  $J_\infty$  than in the low ionic strength case. According to Tables 6 and 7,  $1/b$

decreased with the increase of NaCl concentration, especially in the range of 0.03%–0.06% w/w, which decreased by 5.13% per 0.01% increase in the NaCl concentration (Table 7). Herrero et al. [17] reported higher saline content in BSA solution resulted in the faster flux decay. The value of  $K_c$ ,  $K_f$ ,  $K_s$  and  $K_{cf}$  increased with increase in NaCl concentration, while complete blocking was the main blocking mechanism followed by intermediate blocking at all NaCl concentrations (Table 5). On the other hand, the  $K_{cf}$  was the most sensitive fouling constant to the NaCl concentration and showed the maximum increasing percentage per 0.01% increase in the NaCl concentration (Table 7).

#### 4.7. Sensitivity analysis

Sensitivity analysis (SA) is defined as the study of the uncertainty of the output relative to the uncertainty of different inputs to identify the relevant input factors [29]. Among several methods of SA (e.g., scatter plot, ANOVA and variance-based), regression analysis method was conducted in this study. Regression analysis, in the context of SA, contains fitting a linear regression to the model response and uses standardized regression coefficients as a direct measurement of sensitivity. As given in Table 8, NaCl concentration was the most effective factor in the dynamic permeate flux of milk UF process, while, flow rate had the lowest effect on it. In addition, SA of HKM model parameters revealed that TMP and temperature were two variables with the highest impact on  $a$  parameter, whereas flow rate showed the least impact on this parameter.  $1/b$  was mainly affected by NaCl concentration and temperature, while pH showed the slight effect on flux decline rate. Among input variables, TMP showed the highest impact on  $J_0$  and the lowest impact on  $J_\infty$ . The initial flux was almost unaffected by flow rate. In addition, pH showed the highest effect on  $K_c$  and  $K_f$ , whereas, NaCl demonstrated the highest impact on  $K_{cf}$  and  $K_s$ .

### 5. Conclusion

Process modeling plays a very important role in membrane operation of colloidal suspensions such as skim milk. Herein, we applied three models including, exponential kinetic,  $n$ -order kinetic and HKMs to better understand the mechanisms of permeate flux decline in UF of skim milk at

Table 8

Sensitivity analysis of the parameters of homographic kinetic and Hermia's models and the input variables applied in crossflow ultrafiltration of skim milk

Parameters	$J_i$ (kg/h × m <sup>2</sup> )	$a$	$1/b$ (min)	$J_0$ (kg/h × m <sup>2</sup> )	$J_\infty$ (kg/h × m <sup>2</sup> )	$K_c$ (s <sup>-1</sup> )	$K_s$ (s <sup>-0.5</sup> m <sup>-0.5</sup> )	$K_f$ (m <sup>-1</sup> )	$K_{cf}$ (s m <sup>-2</sup> )
TMP (1 bar)	0.44	0.47	-0.38	0.66	0.2	0.47	0.41	0.52	0.72
$T$ (°C)	0.25	0.43	-0.51	0.37	0.29	0.35	0.68	-0.32	0.53
FR (L/min)	0.2	-0.1	0.28	0.07	0.22	-0.29	0.37	-0.41	-0.37
pH	0.29	-0.27	-0.07	0.25	0.37	-0.82	-0.51	-0.65	-0.53
NaCl (%)	-0.50	0.20	-0.57	-0.28	-0.61	0.51	-0.78	0.46	0.83
Time (min)	-0.38	-	-	-	-	-	-	-	-

$a$ , flux decline extent;  $1/b$ , flux decline time constant;  $J_f$ , dynamic flux,  $J_0$ , initial flux,  $J_\infty$ , steady-state flux.

different operational conditions. The results indicated that all three mentioned models were highly significant for modeling the dynamic permeate flux of skim milk, but from the point of being in better agreement with the experimental data, homographic kinetic model, which has not been used for the description of membrane filtration processes so far, did the best. From the results obtained in this paper, the effect of operating conditions (TMP, FR, ionic strength, temperature and pH) played an important role in flux pattern. Increasing the temperature, TMP, FR and pH led to an increase in both the initial and steady-state fluxes, whereas the increase in ionic strength repressed these parameters. Increasing the temperature, FR and pH resulted in lower extent of flux decline, but the increase in TMP and ionic strength enhanced this parameter. In addition, the rate of flux decline reduced by increasing FR and enhanced by increasing the temperature, TMP, pH and ionic strength. SA indicated that among the input variables, NaCl concentration was the most sensitive factor on dynamic flux,  $1/b$  and  $J_{\infty}$ , while TMP showed the most impact on  $a$  and  $J_0$  parameters. Furthermore, Hermia's models were used to analyze the blocking mechanisms occurred in the flux decline of skim milk UF. The models fitted well to the experimental data and the best fit to the experimental data corresponded to the pore blocking model followed by cake layer formation for all the experimental conditions tested. Although, it was observed that different blocking mechanisms may take place during the UF process which led the combination of two or more in the process. The values of  $K_c$ ,  $K_f$ ,  $K_s$  and  $K_{cf}$  increased with increase in TMP, temperature and NaCl concentration, indicating conditions that led to more severe fouling of the membranes. On the other hands, the values of these parameters decreased as pH and FR increased, except of  $K_i$  for temperature, which decreased as temperature increased. Furthermore, NaCl concentration showed the most impact on  $K_{cf}$  and  $K_s$  and pH showed the most influence on  $K_c$  and  $K_f$ . This also implied that the cleaning procedure for the membrane fouled with skim milk under these experimental conditions must be selected based on the predominant types of fouling which were complete blocking followed by intermediate and standard blocking for all the operational conditions and feed solutions tested. This new insight to dynamic flux modeling is useful to characterize the fouling behavior of any colloidal suspensions.

## References

- [1] M. Cheryan, Ultrafiltration, I.D. Wilson, E.R. Adlard, M. Cooke, C.F. Poole, Eds., Encyclopedia of Separation Science, Academic Press, NY, 2000.
- [2] N. Iakovchenko, L. Silantjeva, Vegetable ingredients in soft cheese made from concentrated skim milk by ultrafiltration, *Agron. Res.*, 12 (2014) 717–726.
- [3] W.R. Bowen, F. Jenner, Dynamic ultrafiltration model for charged colloidal dispersions: a Wigner-Seitz cell approach, *Chem. Eng. Sci.*, 50 (1995) 1707–1736.
- [4] A.M.St. John, R.W. Cattrall, S.D. Kolev, Determination of the initial flux of polymer inclusion membranes, *Sep. Purif. Technol.*, 116 (2013) 41–45.
- [5] R.W. Field, D. Wu, J.A. Howell, B.B. Gupta, Critical flux concept for microfiltration fouling, *J. Membr. Sci.*, 100 (1995) 259–272.
- [6] A. Alghooneh, S.M.A. Razavi, S.M. Mousavi, Nanofiltration treatment of tomato paste processing wastewater: process modeling and optimization using response surface methodology, *Desal. Wat. Treat.*, 57 (2015) 9609–9621.
- [7] M. Cinta Vincent Vela, S. Álvarez Blanco, J. Lora García, E. Bergantiños Rodríguez, Analysis of membrane pore blocking models applied to the ultrafiltration of PEG, *Sep. Purif. Technol.*, 62 (2008) 489–498.
- [8] K. Masoudnia, A. Raisi, A. Aroujalian, M. Fathizadeh, Treatment of oily wastewaters using the microfiltration process: effect of operating parameters and membrane fouling study, *Sep. Purif. Technol.*, 48 (2013) 1544–1555.
- [9] A.S. Cassini, I.C. Tessaro, L.D.F. Marczak, Ultrafiltration of wastewater from isolated soy protein production: fouling tendencies and mechanisms, *Sep. Purif. Technol.*, 46 (2011) 1077–1086.
- [10] T.E. Clarke, C.A. Heath, Ultrafiltration of skim milk in flat-plate and spiral-wound modules, *J. Food Eng.*, 33 (1997) 373–383.
- [11] S.M.A. Razavi, S.M. Mousavi, S.A. Mortazavi, Dynamic prediction of milk ultrafiltration performance: a neural network approach, *Chem. Eng. Sci.*, 58 (2003) 4185–4195.
- [12] S.M.A. Razavi, S.M. Mousavi, S.A. Mortazavi, Application of neural networks for crossflow milk ultrafiltration simulation, *Int. Dairy J.*, 14 (2004) 69–80.
- [13] A. Naik, S.N. Raghavendra, K.S.M.S. Raghavarao, Production of coconut protein powder from coconut wet processing waste and its characterization, *Appl. Biochem. Biotechnol.*, 167 (2012) 1290–1302.
- [14] N.S. Krishna Kumar, M.K. Yea, M. Cheryan, Ultrafiltration of soy protein concentrate: performance and modeling of spiral and tubular polymeric modules, *J. Membr. Sci.*, 244 (2004) 235–242.
- [15] R.S. Faibish, M. Elimelech, Y. Cohen, Effect of interparticle electrostatic double layer interactions on permeate flux decline in crossflow membrane filtration of colloidal suspensions: an experimental investigation, *J. Colloid Interface Sci.*, 204 (1998) 77–86.
- [16] S. Hong, R.S. Faibish, M. Elimelech, Kinetics of permeate flux decline in crossflow membrane filtration of colloidal suspensions, *J. Colloid Interface Sci.*, 196 (1997) 267–277.
- [17] C. Herrero, P. Pradanos, J.I. Calvo, F. Tejerina, A. Hernandez, Flux decline in protein microfiltration: influence of operative parameters, *J. Colloid Interface Sci.*, 187 (1997) 344–351.
- [18] K.F. Eckner, E.A. Zottola, Modeling flux of skim milk as a function of pH, acidulant and temperature, *J. Dairy Sci.*, 75 (1992) 2952–2958.
- [19] H. Nourbakhsh, Z. Emam-Djomeh, H. Mirsaeedghazi, M. Omid, S. Moieni, Study of different fouling mechanisms during membrane clarification of red plum juice, *Int. J. Food Sci. Technol.*, 48 (2013) 58–64.
- [20] A. Grandison, W. Youravong, M.J. Lewis, Hydrodynamic factors affecting flux and fouling during ultrafiltration of skimmed milk, *Le Lait*, 80 (2000) 165–174.
- [21] D.M. Krstić, M.N. Tekić, M.D. Carić, D. Milanović, The effect of turbulence promoter on cross-flow microfiltration of skim milk, *J. Membr. Sci.*, 208 (2002) 303–314.
- [22] P.F. Fox, *Advanced Dairy Chemistry – 1: Proteins*, Elsevier Applied Science, New York, NY, 1992.
- [23] H.G. Ramachandra Rao, Mechanisms of flux decline during ultrafiltration of dairy products and influence of pH on flux rates of whey and buttermilk, *Desalination*, 144 (2002) 319–324.
- [24] R.L. Brandsma, S.S.H. Rizvi, Depletion of whey proteins and calcium by microfiltration of acidified skim milk prior to cheese making, *J. Dairy Sci.*, 82 (1999) 2063–2069.
- [25] P. Walstra, R. Jenness, *Dairy Chemistry and Physics*. John Wiley & Sons, Inc., New York, NY, 1984.
- [26] A.O. Karlsson, R. Ipsen, K. Schrader, Y. Ardo, Relationship between physical properties of casein micelles and rheology of skim milk concentrate, *J. Dairy Sci.*, 88 (2005) 3784–3797.
- [27] Y.X. Yu, G.H. Gao, Y.G. Li, Surface tension for aqueous electrolyte solutions by the modified mean spherical approximation, *Fluid Phase Equilib.*, 173 (2000) 23–38.
- [28] D.N. Petsev, V.M. Starov, I.B. Ivanov, Concentrated dispersions of charged colloidal particles: sedimentation, ultrafiltration and diffusion, *Colloids Surf.*, A, 81 (1993) 65–81.
- [29] A. Saltelli, A. Tarantola, F. Campolongo, M. Ratto, *Sensitivity Analysis in Practice*, Wiley, New York, NY, 2004.